*Aust. J. Phys.*, 1976, **29**, 273–88

# Extended Theory of Magnon Sideband Shapes. I Impure Three-dimensional Ferromagnets

*D. D. Richardson*

Department of Theoretical Physics, Research School of Physical Sciences, Australian National University; present address: Department of Physics, Cavendish Laboratory, Madingley Road, Cambridge CB3 OHE, U.K.

*Abstract*

A calculation of magnon sideband lineshapes is given which uses a simple phenomenological Hamiltonian allowing of an exact solution. The perturbation Hamiltonian has an improved form compared with that used by Richardson (1974). We consider the effect of a small concentration of substitutional spin impurities on the sideband. An example of an f.c.c. ferromagnetic crystal is studied in detail, and the conditions for the appearance of local modes due to the impurity are discussed. The possibility of resonance modes occurring within the absorption band is considered but, for the f.c.c. crystal studied here, this appears to be unlikely to within the accuracy of the numerical calculations undertaken.

## 1. Introduction

In a previous paper (Richardson 1974, referred to hereafter as Paper I) the author presented a simple model for calculating magnon sideband lineshapes in impure ferromagnetic crystals. A model of this type is discussed further in the present paper, but here a more realistic form is taken for the perturbation Hamiltonian describing the interaction of the crystal with an applied electric field. We apply the model to a three-dimensional f.c.c. crystal and discuss the predicted magnon sideband lineshape and how this will be affected by a substitutional spin impurity.

As in Paper I, we take a model Hamiltonian with Frenkel-type excitons and include a quadratic form of exciton–magnon interaction. The model crystal Hamiltonian adopted has the form

$$\mathscr{H}_0 = \sum_k \varepsilon_1(\boldsymbol{k})\, a_k^+ a_k + \sum_k \varepsilon_2\, b_k^+ b_k + g \sum_k (a_k^+ b_k + b_k^+ a_k) + \gamma N^{-1} \sum_{k,k'} a_k^+ a_{k'}, \quad (1)$$

where $a_k^+$ and $b_k^+$ are magnon and exciton creation operators respectively, and the sums over $\boldsymbol{k}$ are over the first Brillouin zone of the lattice. The first term of equation (1) represents the magnon Hamiltonian of the crystal. The magnon energy $\varepsilon_1(\boldsymbol{k})$ is given for a ferromagnet by

$$\varepsilon_1(\boldsymbol{k}) = 2|J|Sz(1-\gamma_k) - z|J|S^2\rho, \quad (2)$$

where

$$\gamma_k = z^{-1} \sum_{[\Delta]} \exp(\mathrm{i}\boldsymbol{k}.\Delta) \qquad \text{and} \qquad \rho = J'S'/JS - 1, \quad (3a, b)$$

with $J$ and $S$ the pure crystal exchange integral and spin, and $J'$ and $S'$ the corresponding values for the impurity. The sum over $\Delta$ in equation (3a) is over all nearest neigh-

bour sites of any magnetic ion and $z$ is the number of nearest neighbours. The last term of equation (2) is a constant due to the impurity and will only have the effect of shifting the entire spectrum by that amount. We therefore ignore it in what follows.

The second term of equation (1) represents the exciton part of the Hamiltonian. Because of the observation that the high-energy cutoff of the magnon sideband is very close to $\varepsilon_1(\boldsymbol{k})|_{\max}$ (see e.g. Stevenson 1966; or, more recently, Srivastava and Stevenson 1972; Srivastava *et al.* 1973) and also the general fact that the dispersion of the exciton energy is small, we assume that any such dispersion has a negligible effect on the magnon sideband. We therefore choose the exciton energy $\varepsilon_2$ to be independent of wavenumber.

The third term of equation (1) gives a form of the exciton–magnon interaction in the crystal. A more rigorous four-operator form has been given, e.g. by Eremenko *et al.* (1974), and has also been used in the calculations of Parkinson and Loudon (1968) and Moriya and Inoue (1968). All these authors found it necessary to make some approximations when evaluating Green's functions from the four-operator form, and it may be readily shown that the quadratic form used here is an approximation to the more rigorous form obtained by using their decoupling methods. We therefore avoid the need for making decoupling approximations in our Green's functions by the choice of our quadratic form. As is pointed out in Section 2, the present simple model calculations can give results very similar to those of the more sophisticated model of Parkinson and Loudon (1968) if the exciton–magnon interaction strength $g$ is given some $\boldsymbol{k}$ dependence.

The last term of equation (1) describes the effect of an impurity on the crystal. A rigorous expression for the impurity parameter $\gamma$ as a function of $\boldsymbol{k}$ and $\boldsymbol{k}'$ has been given by Callaway (1963). For the present case where we take $\gamma$ to be $\boldsymbol{k}$ independent, we find that it may be approximated as

$$\gamma \approx 2|J|Sz\varepsilon \qquad \text{for} \qquad \varepsilon = J'/J - 1 . \tag{4a, b}$$

From the form of the impurity term it will be observed that the impurity will cause scattering of magnons with wavenumber $\boldsymbol{k}$ into those with wavenumber $\boldsymbol{k}'$, and thus we expect a perturbation of the density of states of the crystal. For a pure crystal the density of states is given by

$$\mathfrak{g}_0(\lambda) = N^{-1} \sum_{\boldsymbol{k}} \delta(\varepsilon_1(\boldsymbol{k}) - \lambda), \tag{5}$$

while for an impure crystal the density of states is given by (Paper I)

$$\mathfrak{g}(\lambda) = \mathfrak{g}_0(\lambda) - \frac{1}{\pi} \operatorname{Im}\left(\frac{\mathrm{d}\ln(\mathscr{D}(\lambda))}{\mathrm{d}\lambda}\right), \tag{6}$$

where

$$\mathscr{D}(\lambda) = 1 + \gamma N^{-1} \sum_{\boldsymbol{k}} \{\varepsilon_1(\boldsymbol{k}) - \lambda\}^{-1} \tag{7}$$

arises from the secular determinant of the magnon and impurity Hamiltonians.

We may write equation (7) in terms of real and imaginary parts by giving $\lambda$ a small imaginary part and using Dirac's relation

$$\lim_{\varepsilon \to 0+} (x \pm \mathrm{i}\varepsilon)^{-1} = \mathrm{P}/x \mp \mathrm{i}\pi\delta(x), \tag{8}$$

where P denotes the principal part of the integral. Then we write

$$\mathscr{D}(\lambda) = 1 + \gamma R(\lambda) + i\pi\gamma\, g_0(\lambda) \tag{9}$$

using equation (5) and defining

$$R(\lambda) = (P/V^*) \int_{V^*} \{\varepsilon_1(\boldsymbol{k}) - \lambda\}^{-1}\, d\boldsymbol{k}, \tag{10}$$

where we have changed the sum to an integral over the first Brillouin zone of volume $V^*$. The function $R(\lambda)$ is the Hilbert transform of $g_0(\lambda)$.

If we define a function $\delta(\lambda)$ such that (Callaway 1974)

$$\tan(\delta(\lambda)) = -\pi\gamma\, g_0(\lambda)/\{1 + \gamma R(\lambda)\}, \tag{11}$$

it can be shown that equation (6) for the density of states may be written

$$g(\lambda) = g_0(\lambda) - (\pi\eta)^{-1}\, d\delta/d\lambda, \tag{12}$$

where $\eta$ is the number of unit cells in the crystal. If there are a small number $n$ of impurities, their effects may be added. We therefore obtain for the change in density of states due to the impurity

$$\Delta g(\lambda) = -(c/\pi)\, d\delta/d\lambda, \tag{13}$$

where $c = n/\eta$. It should be noted that there is an error in the case of a one-dimensional crystal, as described in Paper I, where the absolute value of the derivative was taken. Since the total number of states in the system is conserved, if there is an increase in the density of states in one region there must be decreases elsewhere.

The perturbation Hamiltonian used in Paper I to describe the interaction of the crystal with an applied electric field represents only a very simple approximation to the correct Hamiltonian. This may be seen from the observation that in most crystals the parent exciton has a different dipole character from that of the magnon sideband, so that for an electric dipole sideband (as most commonly observed) the parent exciton will be magnetic dipole in nature and will not couple with an electric field. This point has been discussed in more detail by Richardson (1976).

A more exact form of perturbation Hamiltonian would take into account both the excitons and magnons together. We here choose a form which has been used by many authors. It is analogous to the Hamiltonian first discussed by Tanabe *et al.* (1965) for indirect exchange coupling between excitons and magnons in the presence of the field, and to the Hamiltonian proposed by Halley and Silvera (1965) for direct electromagnetic coupling, although the magnitudes of these two types of interaction may be quite different. That is, we take the perturbation as

$$\mathscr{H}_p = l \sum_k (a_k^+ b_k^+ + a_k b_k), \tag{14}$$

where $l$ is the time-dependent strength of the perturbation and includes the strength of the applied field. It is expected that the perturbation Hamiltonian (14) will give a more realistic description of magnon sideband lineshapes than that given by the Hamiltonian of Paper I.

The present calculations represent the absorption of a single polarization direction in the crystal by a particular polarization of the applied field. That is, we obtain the result for a particular component of the optical absorption tensor (Richardson 1976)

$$\alpha_{\eta\nu}(\omega) = -\tfrac{1}{2}\omega \operatorname{Im}\big(G_{\eta\nu}(\omega)\big), \tag{15}$$

where the dyadic Green's function is defined by the time Fourier transform of

$$\begin{aligned} G_{\eta\nu}(t-t') &= \langle\langle p_\eta(t-t'), p_\nu(0)\rangle\rangle \\ &= -\{\hbar Z(\beta)\}^{-1} \operatorname{Tr}\big(\exp(-\beta\mathscr{H}_0)[p_\eta(t-t'), p_\nu(0)]\big)\,\theta(t). \end{aligned} \tag{16}$$

Here $p_\eta$ is the $\eta$th component of the crystal dipole moment, $Z(\beta)$ is the canonical partition function, $\beta = 1/k_B T$ with $k_B$ Boltzmann's constant and $T$ the temperature, $\theta(t)$ is a stepfunction which is unity for $t > 0$ and zero for $t < 0$, and $[p_\eta(t-t'), p_\nu(0)]$ represents the commutator of $p_\eta$ and $p_\nu$. In the present case we are therefore interested in evaluating the Green's functions

$$G(\omega) = \langle\langle a_k^+ b_k^+ + a_k b_k, a_{k'}^+ b_{k'}^+ + a_{k'} b_{k'}\rangle\rangle_\omega, \tag{17}$$

where the Green's function on the right-hand side has been time Fourier-transformed, making use of the Hamiltonian (14), where the operators in the sum represent the crystal polarization due to the applied field (Moriya 1968).

## 2. Calculations

The crystal Hamiltonian (1) was diagonalized in Paper I, which should be referred to for details. The result of the diagonalization is that equation (1) may be written as

$$\mathscr{H}_0 = \sum_\lambda \{\lambda^+(\lambda) C_{1\lambda}^+ C_{1\lambda} + \lambda^-(\lambda) C_{2\lambda}^+ C_{2\lambda}\}, \tag{18}$$

where the new operators $C_{1\lambda}$ and $C_{2\lambda}$ are defined by

$$C_{1\lambda} = \frac{\{2Y(Y+X)\}_\lambda^{-\frac{1}{2}}}{\mathscr{N}_\lambda} \sum_k \frac{a_k}{\varepsilon_1(\boldsymbol{k})-\lambda} + \frac{\{(Y+X)/2Y\}_\lambda^{\frac{1}{2}}}{\mathscr{N}_\lambda} \sum_k \frac{b_k}{\varepsilon_1(\boldsymbol{k})-\lambda}, \tag{19a}$$

$$C_{2\lambda} = \frac{\{2Y(Y-X)\}_\lambda^{-\frac{1}{2}}}{\mathscr{N}_\lambda} \sum_k \frac{a_k}{\varepsilon_1(\boldsymbol{k})-\lambda} - \frac{\{(Y-X)/2Y\}_\lambda^{\frac{1}{2}}}{\mathscr{N}_\lambda} \sum_k \frac{b_k}{\varepsilon_1(\boldsymbol{k})-\lambda} \tag{19b}$$

and

$$\lambda^\pm(\lambda) = \tfrac{1}{2}(\varepsilon_2+\lambda) \pm g\,Y(\lambda), \tag{20}$$

for

$$\mathscr{N}_\lambda^2 = \sum_k \{\varepsilon_1(\boldsymbol{k})-\lambda\}^{-2}, \quad X(\lambda) = \frac{(\varepsilon_2-\lambda)}{2g}, \quad Y(\lambda) = [X^2(\lambda)+1]^{\frac{1}{2}}. \tag{21a, b, c}$$

The eigenvalue $\lambda$ of the magnon and impurity parts of the Hamiltonian is obtained from solutions of the secular equation

$$\mathscr{D}(\lambda) = 1 + (\gamma/N) \sum_k \{\varepsilon_1(\boldsymbol{k})-\lambda\}^{-1} = 0. \tag{22}$$

In the limit as the exciton–magnon interaction strength $g$ goes to zero, $\lambda^+ \to \varepsilon_2$ and $\lambda^- \to \lambda$, so that for $g$ nonzero we have an exciton-like branch represented by the operators $C_{1\lambda}$ and a magnon-like branch represented by the operators $C_{2\lambda}$. Since it is readily shown that $C_{1\lambda}$ and $C_{2\lambda}$ satisfy boson commutation rules and commute with each other, we may consider the excitation modes of $C_{1\lambda}$ and $C_{2\lambda}$ as being new elementary excitations having both some magnon and some exciton character.

We may use the inverse relationships to the equations (19) to rewrite the perturbation Hamiltonian (14) in terms of the new operators for which the crystal Hamiltonian is diagonal. The result is

$$\mathscr{H}_{\mathrm{p}} = l \sum_{\lambda} \left[\{2Y(\lambda)\}^{-1}\{C_{1\lambda}^{+} C_{1\lambda}^{+} + C_{1\lambda} C_{1\lambda} - (C_{2\lambda}^{+} C_{2\lambda}^{+} + C_{2\lambda} C_{2\lambda})\}\right.$$
$$\left. + \{X(\lambda)/Y(\lambda)\}(C_{1\lambda}^{+} C_{2\lambda}^{+} + C_{1\lambda} C_{2\lambda})\right]. \tag{23}$$

We may now evaluate the Green's functions (17). There are only three nonzero ones, and we shall see how they are obtained by evaluating one of them explicitly. We treat the Green's function

$$\langle\langle C_{1\lambda} C_{2\lambda}, C_{1\lambda'}^{+} C_{2\lambda'}^{+}\rangle\rangle. \tag{24}$$

This has an equation of motion in time Fourier transform as

$$\hbar\omega\langle\langle C_{1\lambda} C_{2\lambda}, C_{1\lambda'}^{+} C_{2\lambda'}^{+}\rangle\rangle = \langle[C_{1\lambda} C_{2\lambda}, C_{1\lambda'}^{+} C_{2\lambda'}^{+}]\rangle + \langle\langle[C_{1\lambda} C_{2\lambda}, \mathscr{H}_0], C_{1\lambda'}^{+} C_{2\lambda'}^{+}\rangle\rangle, \tag{25}$$

where the first term on the right-hand side is the average equal-time commutator. The commutator of the Green's function on the right-hand side of equation (25) may be evaluated to give

$$\langle\langle[C_{1\lambda} C_{2\lambda}, \mathscr{H}_0], C_{1\lambda'}^{+} C_{2\lambda'}^{+}\rangle\rangle = \{\lambda^{+}(\lambda) + \lambda^{-}(\lambda)\}\langle\langle C_{1\lambda} C_{2\lambda}, C_{1\lambda'}^{+} C_{2\lambda'}^{+}\rangle\rangle, \tag{26}$$

while the equal-time commutator gives

$$\langle[C_{1\lambda} C_{2\lambda}, C_{1\lambda'}^{+} C_{2\lambda'}^{+}]\rangle = \langle C_{1\lambda}, C_{1\lambda'}^{+}\rangle \delta(\lambda, \lambda') + \langle C_{2\lambda'}^{+}, C_{2\lambda}\rangle \delta(\lambda, \lambda') = \delta(\lambda, \lambda') \tag{27}$$

since from equation (19b) we have

$$C_{2\lambda}|0\rangle = 0. \tag{28}$$

Therefore equation (25) may be solved exactly to give

$$\langle\langle C_{1\lambda} C_{2\lambda}, C_{1\lambda'}^{+} C_{2\lambda'}^{+}\rangle\rangle = \delta(\lambda, \lambda')/[\hbar\omega - \{\lambda^{+}(\lambda) + \lambda^{-}(\lambda)\}]$$
$$= \delta(\lambda, \lambda')/\{\hbar\omega - (\varepsilon_2 + \lambda)\} \tag{29}$$

by making use of equation (20). The other nonzero Green's functions are

$$\langle\langle C_{1\lambda} C_{1\lambda}, C_{1\lambda'}^{+} C_{1\lambda'}^{+}\rangle\rangle = \delta(\lambda, \lambda')/\{\hbar\omega - 2\lambda^{+}(\lambda)\}, \tag{30a}$$

$$\langle\langle C_{2\lambda} C_{2\lambda}, C_{2\lambda'}^{+} C_{2\lambda'}^{+}\rangle\rangle = \delta(\lambda, \lambda')/\{\hbar\omega - 2\lambda^{-}(\lambda)\}. \tag{30b}$$

The optical absorption lineshape (equation 15) will be given from the imaginary parts of equations (29) and (30) by

$$\alpha(\omega) \approx -\tfrac{1}{2}\omega \sum_{\lambda} \left[\{X^2(\lambda)/Y^2(\lambda)\}\delta(\hbar\omega-(\varepsilon_2+\lambda)) + \{4Y^2(\lambda)\}^{-1}\{\delta(\hbar\omega-2\lambda^+(\lambda)) + \delta(\hbar\omega-2\lambda^-(\lambda))\}\right]. \quad (31)$$

It will be seen from equation (31) that the second and third terms on the right-hand side give the two-exciton and two-magnon absorption lines when there is an exciton–magnon interaction present. Note that the lines are shifted from their $g = 0$ frequencies by the interaction, as well as being modified in shape from the single excitation lineshape by the factor $\{4Y^2(\lambda)\}^{-1}$.

The magnon sideband lineshape is given by the first term of equation (31), i.e. the absorption lineshape is given by

$$\begin{aligned}\alpha(\omega) &\approx -\tfrac{1}{2}\omega N^{-1} \sum_{\lambda} \left[(\varepsilon_2-\lambda)^2/\{(\varepsilon_2-\lambda)^2+4g^2\}\right]\delta(\hbar\omega-(\varepsilon_2+\lambda)) \\ &\approx -2\pi\omega \int \left[(\varepsilon_2-\lambda)^2/\{(\varepsilon_2-\lambda)^2+4g^2\}\right]\delta(\hbar\omega-(\varepsilon_2+\lambda))\, \mathfrak{g}(\lambda)\, d\lambda \\ &\approx -2\pi\omega\left[(2\varepsilon_2-\hbar\omega)^2/\{(2\varepsilon_2-\hbar\omega)^2+4g^2\}\right]\mathfrak{g}(\hbar\omega-\varepsilon_2), \end{aligned} \quad (32)$$

where $\mathfrak{g}(\hbar\omega-\varepsilon_2)$ is the impure magnon density of states given by equation (6) or (12).

The calculated magnon sideband thus has the following properties (from equation 32):

(1) It lies on the high energy side of the parent exciton frequency $\varepsilon_2$ (not shown here as it is not considered as coupling to the electric field).

(2) It has a bandwidth of $\varepsilon_1(\boldsymbol{k})_{\max} = \varepsilon_0$.

(3) It has the shape of the magnon density of states modified by a function dependent on the exciton–magnon interaction strength $g$.

(4) The low energy edge of the band is at $\varepsilon_2$. In reality the band may be shifted slightly from this lower limit by the exciton–magnon interaction, as pointed out by Parkinson and Loudon (1968), although such a shift should be quite small.

The dependence of the sideband lineshape on the exciton–magnon interaction occurs through the term

$$f(g,\omega) = (2\varepsilon_2-\hbar\omega)^2/\{(2\varepsilon_2-\hbar\omega)^2+4g^2\}. \quad (33)$$

To discuss what values of $g$ have the greatest effect on the lineshape (equation 32), we consider $f(g,\omega)$ as a function of $g$. It has a maximum of unity at $g = 0$, and a point of inflection at

$$g = (\varepsilon_2-\tfrac{1}{2}\hbar\omega)/\sqrt{3} \approx (\varepsilon_2-\varepsilon_0)/2\sqrt{3} \quad (34)$$

when $f(g,\omega) = 0{\cdot}75$. Since in general $\varepsilon_2 \gg \varepsilon_0$ the point of inflection occurs far from the origin and $f(g,\omega)$ will be slowly varying for all values of $g$ and $\omega$. In the neighbourhood of the point of inflection $f(g,\omega)$ is nearly linear and has a maximum slope of approximately $\frac{3}{8}(\varepsilon_2-\varepsilon_0)^{-1}$, which is small. We therefore conclude that the function

$f(g, \omega)$ will have little effect on the lineshape for any value of $g$ though, for increasing values of $g$, the magnitude of the absorption will be reduced.

The above conclusions do not agree with the calculations of Parkinson and Loudon (1968) who found that the exciton–magnon interaction had a significant effect on the lineshape, causing the maximum of the antiferromagnetic perovskite crystal density of states to shift from the edge of the band, and to become finite. It is felt that the reason for this difference is due to the omission of a $\boldsymbol{k}$ dependence of $g$, which may be too rough an approximation. If we give $g$ some $\boldsymbol{k}$ dependence, it is simple to show that for the pure crystal case we can obtain a form for the sideband lineshape like that of the first line of equation (32) with $g$ replaced by $g(\boldsymbol{k})$, $\lambda$ replaced by $\varepsilon_1(\boldsymbol{k})$ and the sum over $\lambda$ by a sum over $\boldsymbol{k}$. This is then a weighted density-of-states expression, and would give the behaviour discussed by Parkinson and Loudon (1968) if $g(\boldsymbol{k})$ were large near the edge of the Brillouin zone. The same conditions would apply for the impure crystal model discussed here, though the simple diagonalization procedure would no longer apply. In principle the calculation can still be done exactly, however. For simplicity we have ignored any $\boldsymbol{k}$ dependence of $g$ in the present calculations, as we are mainly interested in the effect of an impurity on the sideband.

*Example*

It is most straightforward to explain the effects of a substitutional spin impurity on the magnon sideband by discussing an example. Only two reports of magnon sidebands in ferromagnets being observed experimentally have been made. The first report, by Hulin *et al.* (1971), described an emission spectrum of EuO. Since combinations of operators other than those used in the present Hamiltonians are allowed for emission spectra, it is felt that the present model is not adequate to describe or explain this spectrum. The other report, by Meltzer (1972), was on the absorption spectrum of $GdCl_3$. Meltzer indicated that the mechanism of sideband absorption was via a single-ion transition rather than the coupled-ion interaction assumed by the form of our Hamiltonians. It must therefore be concluded that neither of these two experiments is useful for comparison with the present theory. There have been no reports of the effects of impurities on magnon sidebands in ferromagnets. We therefore consider here a hypothetical crystal and investigate all the effects expected due to the impurity.

Because of its cubic symmetry, and hence likely lack of any large anisotropy field, we choose a face-centred cubic (f.c.c.) crystal like EuO. Such a crystal has the magnon energy

$$\varepsilon_1(k) = \tfrac{1}{4}\varepsilon_0[3-\{\cos(\tfrac{1}{2}k_x a)\cos(\tfrac{1}{2}k_y a)+\cos(\tfrac{1}{2}k_y a)\cos(\tfrac{1}{2}k_z a)+\cos(\tfrac{1}{2}k_z a)\cos(\tfrac{1}{2}k_x a)\}], \tag{35}$$

where

$$\varepsilon_0 = 32JS. \tag{36}$$

The pure crystal density of states $g_0(\lambda)$ was calculated using a Monte Carlo method (Buchheit and Loly 1972), and the data from this calculation were used to estimate the shapes of the optical absorption spectrum of the sideband for different values of the exciton–magnon interaction strength $g$. Details of this and other numerical calculations used in the present paper are given in the Appendix.

The f.c.c. density of states has a logarithmic divergence at the high-energy end of the band due to the symmetry points W and X and the points on the interval joining them as shown in Fig. 1 (Loly and Buchheit 1972). There is also a type-I van Hove singularity at 0·75 of the bandwidth due to the point L (Fig. 1) which behaves like

$$\pm(\omega_c-\omega)^{\frac{1}{2}} \quad \text{for} \quad \omega \lesssim \omega_c \qquad \text{and} \qquad \omega-\omega_c \quad \text{for} \quad \omega \gtrsim \omega_c,$$

with $\omega_c$ the cusp-point frequency (Swendsen and Callen 1972).

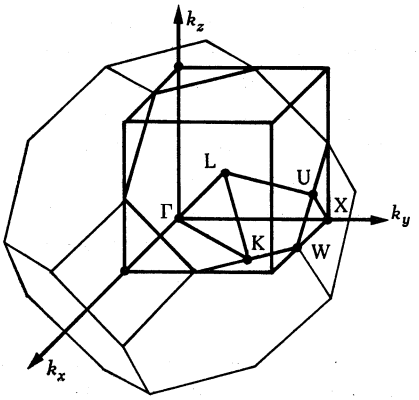


**Fig. 1.** First Brillouin zone of the f.c.c. crystal, showing the irreducible zone bounded by ΓLKWXU, and the cube with side ΓX over which the numerical integrations were taken. The cube contains 12 equivalent irreducible zones.

The numerical calculation does not reproduce well the logarithmic behaviour near the edge of the band, though the trend for the divergence is shown. For a more accurate calculation we would require many more than the $10^6$ values of $\boldsymbol{k}$ that were used, with a resultant large increase in computer time. Since the accuracy of the calculation goes as $N^{\frac{1}{2}}$ for $N$ random numbers, to double the accuracy we require four times the number of points. It is felt that the present calculation with an estimated accuracy of better than 5% overall is adequate for the example we wish to discuss. The Monte Carlo method was chosen because of its versatility especially with calculations in crystals whose unit cells may be combined or transformed into cubes.

Fig. 2 shows the results of calculating the magnon sideband lineshape for different values of the exciton–magnon interaction strength $g$ for the pure crystal ($\gamma = 0$). All the curves were calculated from the same values of the density of states to enable a direct comparison to be made. The parameters used for the examples shown in Fig. 2 are not intended to be realistic values of any transition, but are taken from the transition in EuO discussed by Hulin *et al.* (1971). The values of exciton and magnon energies taken were

$$\varepsilon_2 = 27\,100 \quad \text{cm}^{-1} \qquad \text{and} \qquad \varepsilon_0 = 45 \quad \text{cm}^{-1}. \tag{37}$$

The magnon energy was estimated in two different ways. Barak *et al.* (1974) have given values for the exchange integral ranging from 0·37 to 0·52 $\text{cm}^{-1}$ which, with a spin of $\frac{7}{2}$, may be used in equation (36) to estimate $\varepsilon_0$. Alternatively, McGuire *et al.* (1963) gave an expression for the Curie temperature from molecular field theory as

$$T_c = 8S(S+1)J, \tag{38}$$

which may also be used to estimate $\varepsilon_0$ using the Curie temperature of 69·4 K for EuO and a spin of $\frac{7}{2}$ for the host ions.

It will be seen from Fig. 2 that the intensity of absorption falls as $g$ is increased. This effect is the result of the form of the exciton–magnon Hamiltonian, the third term of equation (1), causing the exciton–magnon pairs induced by the perturbation (14) to be destroyed. The effect can be offset to some extent by the fact that, as $g$ increases, so also would one expect the parameter $l$ to increase in equation (14) since both Hamiltonians are concerned with exciton–magnon interactions. From the slope of $f(g, \omega)$ it is found that, for the same density-of-states data, there is a very slight reduction in the maximum of the edge of the band compared with the intensity at the cusp point at $\varepsilon_2 + 0{\cdot}75\,\varepsilon_0$, though the effect is very small.

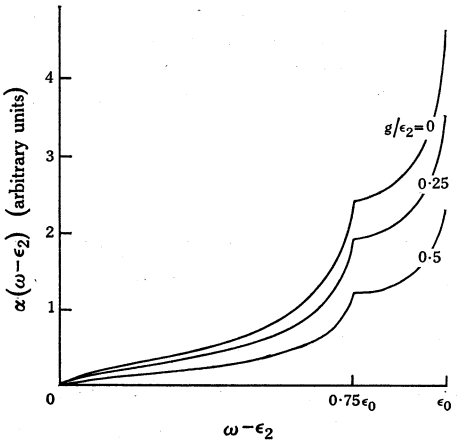


**Fig. 2.** Absorption curves $\alpha(\omega - \varepsilon_2)$ representing magnon sidebands of a pure f.c.c. crystal (such as EuO) for the indicated values of the dimensionless exciton–magnon interaction strength parameter $g/\varepsilon_2$. Note the cusp points at $0{\cdot}75\,\varepsilon_0$.

We now consider the effect of an impurity on the magnon sidebands shown in Fig. 2. It is readily shown that, although the pure crystal density-of-states $\mathfrak{g}_0(\lambda)$ is zero outside the band, the real part of the lattice Green's function is nonzero in this region. It is therefore possible from equations (11) and (12) that the total density-of-states is nonzero at select points outside the band. These will occur when

$$1 + \gamma R(\lambda) = 0. \tag{39}$$

The frequencies $\lambda$ for which equation (39) is satisfied may be found most simply by considering the intersection of the curve of $R(\lambda)$ with $-1/\gamma$. These curves are therefore shown in Fig. 3 for three possible ranges of $\gamma$ which may give some interesting results.

It will be noted that, for values of $\gamma$ which are positive (represented in Fig. 3 by the dashed line A), local modes will occur outside the band on the high-energy side at frequency $\lambda_1$. For small positive values of $\gamma$ the local mode will be very close to the band and may be unobservable. For $\gamma$ negative, but sufficiently large so that

$$|\gamma| > 1/R_1 \tag{40}$$

holds for the point $R_1$ shown in Fig. 3, there will be a local mode at frequency $\lambda_2$ below the band (dashed line B). The local mode will approach the edge of the

band as $\gamma$ approaches $-1/R_1$. A condition such as equation (40) may occur if the impurity–host exchange integral $J'$ is positive (antiferromagnetic coupling) or if $J'$ is sufficiently smaller than $J$ and ferromagnetic. This may be seen by the approximate relation for $\gamma$ in terms of $\varepsilon$ (equation 4a).

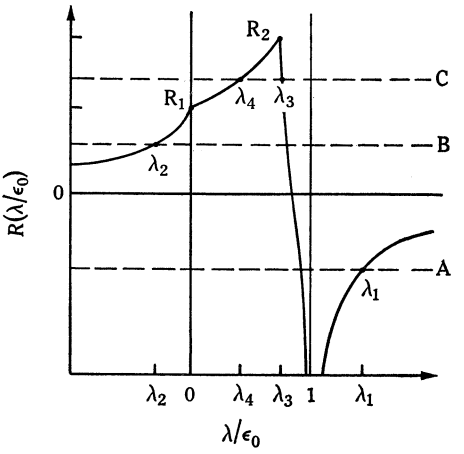


**Fig. 3.** Plot of the real part $R(\lambda)$ of the f.c.c. lattice Green's function both within and without the band $0 < \lambda < 1$. The dashed lines A, B and C represent values of $-1/\gamma$ (see text).

For values of $\gamma$ negative but less than $-1/R_1$ (dashed line C) there can be no local modes, as the curves do not intersect outside the band. For $\gamma$ satisfying the condition

$$-1/R_1 > \gamma > -1/R_2, \tag{41}$$

it may be possible for a 'resonance' mode to occur within the band. That is, the change in the density of states may be large for values $\lambda = \lambda_3$ or $\lambda_4$ shown in the figure. To determine whether a resonance mode will in fact appear, we firstly infer from equation (13) that the change in the density of states must be positive (for a negative change an 'antiresonance' may occur). This alone is not sufficient for the resonance to be observable. Because the change in the density of states is multiplied by the concentration $c$, which is small, the overall effect of the change will be small unless there are large changes at the particular frequencies for resonances. To make this clear, we consider the case when equation (39) is satisfied for $\lambda$ within the band. We may write $1+\gamma R(\lambda)$ as the first term of its Taylor series, i.e.

$$1+\gamma R(\lambda) \approx \gamma(\lambda-\lambda_0)\, R'(\lambda)\,|_{\lambda=\lambda_0}. \tag{42}$$

Then equation (11) becomes

$$\tan\delta \approx -\frac{\pi\gamma\, g_0(\lambda)\,|_{\lambda=\lambda_0}}{\gamma(\lambda-\lambda_0)\, R'(\lambda)\,|_{\lambda=\lambda_0}}. \tag{43}$$

After some manipulation we obtain for the change in the density of states (equation 13)

$$\Delta g(\lambda) = -\tfrac{1}{2}c\Gamma/\{(\lambda-\lambda_0)^2+\tfrac{1}{4}\Gamma^2\}, \tag{44}$$

where the width of the resonance is given by (Callaway 1974)

$$\Gamma = [2\pi\, g_0(\lambda)/R'(\lambda)]_{\lambda=\lambda_0}. \tag{45}$$

Hence, near $\lambda = \lambda_0$ the change in the density of states has a Lorentzian lineshape with a width determined by $\Gamma$ (equation 45). Because of the small factor $c$, $\Delta g(\lambda)$ will only be large near $\lambda = \lambda_0$ if $\Gamma$ is much smaller than unity, so that the width is much narrower than the width of the band, i.e. the conditions for a resonance to occur within the band are

$$|\Gamma| \ll 1 \quad \text{and} \quad \Gamma < 0. \tag{46a, b}$$

We have investigated these conditions numerically for the f.c.c. crystal. It is clear from Fig. 3 that only for points like $\lambda_3$ is the derivative of $R(\lambda)$ negative ($g_0(\lambda)$ is always positive) allowing the condition (46b) to be satisfied, i.e. the range of possible values of $\lambda$ for which it may be possible to have a resonance is (from Fig. 3)

$$0{\cdot}75\,\varepsilon_0 < (\lambda - \varepsilon_2) < \varepsilon_0, \tag{47}$$

since $R(\lambda)$ has a negative slope in this region.

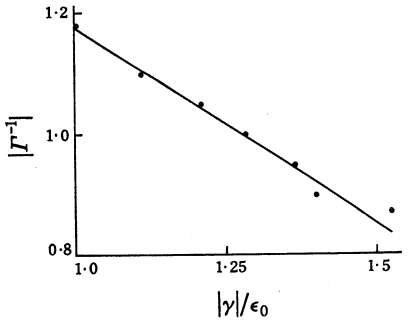


**Fig. 4.** Plot of numerical calculations of possible resonance mode lifetimes $|\Gamma^{-1}|$ for seven values of $\gamma$ satisfying the condition (41), i.e. $-1{\cdot}05 \leqslant \gamma \leqslant -1{\cdot}75$.

Fig. 4 shows the results of the numerical calculation. It is a plot of values of $|\Gamma^{-1}|$, the lifetimes of the resonance mode (which should be much greater than unity for a resonance) against some values of $|\gamma|$ for $\gamma$ negative and satisfying the condition (41). It will be seen that the largest lifetime occurs for $|\gamma|$ just greater than $1/R_2$, as is expected from an inspection of Fig. 3 since $R(\lambda)$ has its greatest slope there, but that the lifetime is not sufficiently large for the resonance to become observable. For values of $\gamma$ which are negative and outside the range of equations (40) and (41) there is no solution to (39) in any region, and we expect there to be no observable effect on the spectrum.

## 3. Conclusions

We have shown in this paper how a simple ferromagnetic model may be solved exactly to give an expression for the shape of a magnon sideband in the absorption spectrum of a crystal. It has been possible to account for the effects of an impurity on the crystal by means of a Koster–Slater type model.

It is found for a wavenumber-independent exciton–magnon interaction strength $g$ that the magnon sideband is proportional to the frequency times the magnon density of states and is approximately independent of the value of $g$, which affects the intensity of absorption but has little effect on the shape. If we were to include a $\boldsymbol{k}$ dependence of $g$ it would be found that for $g(\boldsymbol{k})$ large near the edge of the band that the pure-crystal results of Parkinson and Loudon (1968) could be emulated. For

the impure crystal the matrix diagonalization is no longer simple, but the effect of a $\boldsymbol{k}$-dependent value of $g$ should also be much greater than found here.

The calculated magnon sideband in the present work is found to describe more faithfully the observed properties of sidebands (Hulin *et al.* 1971) than the previous model (Paper I). That is, the sideband can now be shown to exhibit the correct high-energy cutoff energy of $\varepsilon_0$ and width $\varepsilon_0$ also, while the previous model was capable of only describing one or the other of these properties if the parameter $g$ of Paper I was made a free parameter.

Numerical calculations have been made of the magnon sideband lineshape expected from the model for an f.c.c. ferromagnet. The effect of a substitutional spin impurity has been studied in detail, and it is found that for positive values of the impurity parameter $\gamma$ that local modes will occur on the high-energy side of the band. For negative values of $\gamma$ large enough to satisfy the condition (40) it is found that local modes will occur below the band.

The possibility of resonance modes appearing within the band has been investigated for negative values of $\gamma$ satisfying the condition (41). It was found that it is unlikely that resonance modes will occur in f.c.c. ferromagnets within the magnon sideband because it is not possible to satisfy both of the conditions (46) for a resonance.

We therefore conclude that for all values of $\gamma$ which do not allow for the appearance of local modes, the effect of a substitutional impurity will be unobservable. For values of $\gamma$ for which a local mode will appear, it is expected that there will be no observable change to the in-band region, as shown for the pure crystal in Fig. 2. This is because of the small value of the concentration of impurities that we have assumed, and is also a result of Rayleigh's theorems on impurity spectra (Maradudin *et al.* 1971) which show that, when a local mode occurs, the vibration modes within the band cannot change by more than the energy separating the pure crystal modes.

It is felt that the great advantage of the present model over the more complicated antiferromagnetic calculations of Moriya and Inoue (1968), Parkinson and Loudon (1968) and Eremenko *et al.* (1974), who also considered the exciton–magnon interaction, is the fact that the problem may be solved exactly in a straightforward way while still describing the essential features of the observed spectra. The calculation of antiferromagnetic crystal magnon sidebands may also be done simply with a model of this kind (Richardson 1976). The model also allows for improvement by taking a $\boldsymbol{k}$ dependence of the exciton–magnon interaction strength $g$.

Parkinson (1969) has discussed a calculation of the effect of a substitutional spin impurity on an antiferromagnetic crystal magnon sideband. He found similar criteria to the present work for the existence of local modes above the band. He also discussed the occurrence of resonances within the band but concluded that the resonance will be shifted from the solution of $\lambda = \lambda_0$ of equation (39), due to the strong energy dependence of $g_0(\lambda)$ in the region. However, the condition that equation (45) for the resonance width be small can only be met if $g_0(\lambda)$ does not have a strong energy dependence. We therefore expect the resonance to occur at exactly $\lambda = \lambda_0$. The present model therefore, despite its simplicity, is capable of reproducing many of the features of more detailed calculations and has the further advantage of allowing a clear discussion of the existence of resonance modes to be made in a semiqualitative way.

## Acknowledgments

This paper contains part of the work embodied in my thesis as part requirement for qualification for a Ph.D. at the Australian National University. I should like to thank my supervisor Dr J. Mahanty and part-time acting supervisor Dr K. Kumar for their valuable advice during the course of the work. The work would not have been possible without the financial support of a Commonwealth Postgraduate Research Award, supplemented by the Australian National University.

## References

Abramowitz, M., and Stegun, I. A. (1965). 'Handbook of Mathematical Functions', Ch. 5 (Dover: New York).
Anderssen, R. S., and Bloomfield, P. (1974*a*). *Technometrics* **16**, 69–75.
Anderssen, R. S., and Bloomfield, P. (1974*b*). *Numer. Math.* **22**, 157–82.
Barak, J., Gabai, A., and Kaplan, N. (1974). *Phys. Rev.* B **9**, 4914–19.
Buchheit, M., and Loly, P. D. (1972). *Am. J. Phys.* **40**, 289–93.
Byrnes, J. S., Podgor, S., and Zachary, W. W. (1969). *Proc. Cambridge Philos. Soc.* **66**, 377–80.
Callaway, J. (1963). *Phys. Rev.* **132**, 2003–9.
Callaway, J. (1974). 'Quantum Theory of the Solid State', Part B (Academic: New York).
Chadi, D. J., and Cohen, M. L. (1973). *Phys. Rev.* B **8**, 5747–53.
Cooke, J. F., and Wood, R. F. (1972). *Phys. Rev.* B **5**, 1276–83.
Eremenko, V. V., Novikov, V. P., and Petrov, E. G. (1974). *J. Low Temp. Phys.* **16**, 431–54.
Gentleman, W. M., and Sande, G. (1966). *AFIPS Nat. Comput. Conf. Expos. Conf. Proc.* **29**, 563–78.
Gilat, G., and Raubenheimer, L. J. (1966). *Phys. Rev.* **144**, 390–5.
Halley, J. W., and Silvera, I. (1965). *Phys. Rev. Lett.* **15**, 654–6.
Hulin, D., Benoit a la Guillaume, C., and Hanus, J. (1971). Proc. 17th Annual AIP Conf. on Magnetism and Magnetic Materials (Eds C. D. Graham Jr and J. J. Rhyne), No. 5, Part 2, pp. 850–4.
Joyce, G. S. (1971). *J. Phys.* C **4**, L53–6.
Loly, P. D., and Buchheit, M. (1972). *Phys. Rev.* B **5**, 1986–93.
McGuire, T. R., Argyle, B. E., Shafer, M. W., and Smart, J. J. (1963). *J. Appl. Phys.* **34**, 1345–6.
Mahanty, J. (1966). *Proc. Phys. Soc. London* **88**, 1011–14.
Maradudin, A. A., Montroll, E. W., Weiss, G. H., and Ipatova, I. P. (1971). 'Solid State Physics', Suppl. 3, 2nd Ed. (Academic: New York).
Meltzer, R. S. (1972). Proc. 18th Annual AIP Conf. on Magnetism and Magnetic Materials (Eds C. D. Graham Jr and J. J. Rhyne), No. 10, Part 2, pp. 1704–8.
Morita, T. (1975). *J. Phys.* A **8**, 478–89.
Moriya, T. (1968). *J. Appl. Phys.* **39**, 1042–9.
Moriya, T., and Inoue, M. (1968). *J. Phys. Soc. Jpn* **24**, 1251–64.
Mueller, F. M., Garland, J. W., Cohen, M. H., and Bennemann, K. H. (1971). *Ann. Phys. (New York)* **67**, 19–57.
Parkinson, J. B. (1969). *J. Phys.* C **2**, 2003–11.
Parkinson, J. B., and Loudon, R. (1968). *J. Phys.* C **1**, 1568–83.
Ra, O. (1971). *Z. Naturforsch.* **26**, 111–23.
Richardson, D. D. (1974). *Aust. J. Phys.* **27**, 457–70.
Richardson, D. D. (1976). Ph.D. Thesis, Australian National University.
Srivastava, V. C., and Stevenson, R. (1972). *Solid State Commun.* **11**, 41–6.
Srivastava, V. C., Stevenson, R., and Linz, A. (1973). *Solid State Commun.* **13**, 873–6.
Stevenson, R. (1966). *Phys. Rev.* **152**, 531–5.
Swendsen, R. H., and Callen, H. (1972). *Phys. Rev.* B **6**, 2860–75.
Tanabe, Y., Moriya, T., and Sugano, S. (1965). *Phys. Rev. Lett.* **15**, 1023–5.

## Appendix

### *Numerical calculations*

*Pure Crystal Density of States*

There have been many and varied attempts to evaluate numerically the pure crystal density of states (equation 5) in three-dimensional crystals. Joyce (1971) has given an analytic expression for the f.c.c. crystal Green's function in terms of complete elliptic integrals of the first kind. Unfortunately the expression given is too complicated to be of great value in actual computations.

The most common method of estimation until recently was to attempt to calculate series approximations for the integrals involved. For example, Mahanty (1966) and Ra (1971) gave a Fourier series method for calculating the lattice Green's functions, while Byrnes *et al.* (1969) gave a calculation of b.c.c. Green's functions in which they expanded the integrand into a geometric series. Chadi and Cohen (1973) and Morita (1975) made use of special symmetries in the Brillouin zones of cubic crystals to obtain accurate averages over the zone, and to predict values of the lattice Green's function at any point in the zone given its value at certain special points. All methods so far described have the restriction that they must be rederived for each particular crystal of interest, and often there is no guarantee that a method which is successful for one crystal structure will be tractable for any other structure.

One method which is readily adaptable to any crystal whose unit cells may be added or transformed into a cube is that of Monte Carlo type integration using pseudo-random numbers. A good description of the method is given by Buchheit and Loly (1972). Other Monte Carlo calculations using various types of interpolation with improved accuracy for a given computing time have been described by Mueller *et al.* (1971), Gilat and Raubenheimer (1966) and Cooke and Wood (1972). The method described by Buchheit and Loly was used in the present paper to calculate the pure crystal density of states, because of the advantage the method has in its flexibility. The method is described as follows:

In the Brillouin zone of the f.c.c. crystal (Fig. 1) the irreducible zone is the volume bounded by ΓLKWXU. The points within this zone may be transformed by crystal group operations to cover the entire volume of the Brillouin zone. The volume is $\frac{1}{48}$th of the entire Brillouin zone. Such a zone is common to all cubic crystals and greatly simplifies integration over the entire zone, as the total integral is simply 48 times the integral over this volume. For the Monte Carlo calculation we generate points throughout the cube of side ΓX (Fig. 1) in the first octant. This cube contains 12 irreducible zones and the integral will be 4 times the calculated value.

The Monte Carlo method involves generating triplets of random numbers between 0 and 1, multiplying by $\pi$ and evaluating $\varepsilon_1(\boldsymbol{k})$ from equation (35) for the triplet. The range of energies $\lambda$ is divided up into a set of histogram cells, and unity is added to the cell corresponding to the magnitude of $\varepsilon_1(\boldsymbol{k})$. This is repeated until sufficient smoothness of the curve is obtained, the error being proportional to $N^{-\frac{1}{2}}$ for $N$ points generated in the cube.

As also pointed out by Buchheit and Loly (1972) an estimate of the energy at which van Hove singularities occur in the density of states may be made from evaluating the minimum of the group velocity at the energy of each cell. The group velocity is given by

$$\boldsymbol{v}_g = \nabla_k \varepsilon_1(\boldsymbol{k}). \tag{A1}$$

The minimum of $|v_g|$ will go to zero at any van Hove singularity, but is nonzero elsewhere. This procedure is highly sensitive and is valuable for determining singularities near the edges of the zone, or where there is only a slight apparent change in the slope of the curve of density of states at the singularity.

*Impure Crystal Density of States*

The impure density of states is given by equation (12). We must therefore evaluate the function $\delta$ defined by equation (11), which means we require the Hilbert transform (equation 10) of $g_0(\lambda)$ written as

$$R(\lambda) = \frac{\mathrm{P}}{\pi} \int_0^1 \frac{g_0(\lambda')}{\lambda' - \lambda} \, \mathrm{d}\lambda' , \tag{A2}$$

where P signifies the principal part of the integral, and we have taken $g_0(\lambda)$ normalized to be nonzero between 0 and 1.

Equation (10) or (A2) may be evaluated using the Monte Carlo method as for the pure density of states $g_0(\lambda)$, but instead of one cell having a weight of unity for each value of $\boldsymbol{k}$, all cells have a weight for each $\boldsymbol{k}$, the $i$th cell having weight

$$W_i = -\ln\{|(\omega_{i+1} - \omega_m)/(\omega_i - \omega_m)|\} , \tag{A3}$$

where $\omega_i$ is the energy of the $i$th cell, $\omega_m$ is the energy of the cell in which $\varepsilon_1(\boldsymbol{k})$ lies for that particular $\boldsymbol{k}$, and $W_m = 0$. Equation (A3) is just the Hilbert transform of a stepfunction which is unity between $\omega_i$ and $\omega_{i+1}$ and zero elsewhere.

As a consequence of the weight function (A3) the numerical calculations take almost an order of magnitude longer than for the density of states for the same final accuracy. It was therefore considered desirable to find an alternative means of evaluating $R(\lambda)$. The method used follows from considering the Monte Carlo calculation of Buchheit and Loly (1972) with the Fourier series calculation of Mahanty (1966). The pure crystal density of states $g_0(\lambda)$ is evaluated using the Monte Carlo method to the desired accuracy. Use is then made of a numerical fast Fourier transform procedure (Gentleman and Sande 1966) to evaluate the Fourier coefficients $a_n$ of $g_0(\lambda)$. This enables the real part $R(\lambda)$ to be readily calculated since (Mahanty 1966)

$$\begin{aligned} R(\lambda) = \frac{1}{\pi} \sum_n a_n [ & \cos(n\pi\lambda)\{\mathrm{si}(n\pi\lambda) + \mathrm{si}(n\pi(1-\lambda))\} \\ & - \sin(n\pi\lambda)\{\mathrm{ci}(n\pi\lambda) - \mathrm{ci}(n\pi(1-\lambda))\}] , \end{aligned} \tag{A4}$$

where si and ci are the sine and cosine integrals (Abramowitz and Stegun 1965). From the nature of the calculation, the accuracy of $R(\lambda)$ is less than that of $g_0(\lambda)$, particularly near the singularities, where high frequency terms of the Fourier series may be required which will have poor accuracy due to the statistical noise in the evaluated function $g_0(\lambda)$. It is felt that the accuracy is sufficient to describe the essential features of the change in density of states due to the impurity.

The next stage is to evaluate the derivative of $R(\lambda)$ with respect to energy, which is required for equation (45). The differentiation done numerically is very difficult because of the large amount of noise. The method used was developed by Anderssen and Bloomfield (1974*a*, 1974*b*) whose papers give the details of the calculation.

Because of the high noise level, the data are smoothed considerably when differentiated, and there is some distortion of the result, particularly near the singularities. The method is also poor near the ends of the interval. One way to improve on the result is to calculate $g_0(\lambda)$ more accurately so that $R(\lambda)$ is more accurate, but for the present purpose the computation time involved was considered too great. The results for the derivative we have given, however, are within an order of magnitude of the correct values, thus allowing for a semiqualitative discussion of the appearance of resonance modes.

*Local Mode Frequencies*

To determine local mode frequencies we are interested in finding $R(\lambda)$ outside the band. There are several ways in which this may be done. Outside the band there are no singularities, and $R(\lambda)$ may be obtained by direct analytic integration. It may also be found outside the band by the method described in the preceding subsection of this appendix, making use of the Fourier coefficients $a_n$ of $g_0(\lambda)$. It is found that the limits on the accuracy of the coefficients mean that the determination becomes less accurate as one moves away from the band edge. For the f.c.c. crystal the method is good to values of $\lambda$ less than about $1 \cdot 5$ times the width of the band. The method will therefore work only for local modes close to the band (i.e. for $\lambda$ small).

The simplest method of calculating $R(\lambda)$ outside the band is to use the Monte Carlo method described in the previous subsection, with each cell having the weight given by equation (A3). The accuracy of the calculation will be the same over its range of frequencies and can be made as good as desired by increasing computer time. For calculations far removed from the band, the accuracy may be reduced by large differences in equation (A3). Because of the smoothness of the curve and the absence of singularities outside the band, the calculation of $R(\lambda)$ gives far greater accuracy in this region for the same number of random numbers than the calculation inside the band. We therefore decided to use this method to calculate $R(\lambda)$ in the regions outside the band, as shown in Fig. 3.

Although some of the methods mentioned in this appendix give greater accuracy than those chosen for use in the paper, the present methods were selected on the grounds of the ease with which they may be applied to any cubic crystal, and many other crystals as well.

Manuscript received 3 November 1975